Available online at www.sciencedirect.com
ScienceDirect
Ceramics International 37 (2011) 1739–1746
CERAMICS INTERNATIONAL
www.elsevier.com/locate/ceramint

Characterization and oxidation properties of biomorphic porous carbon with SiC gradient coating prepared by PIP method

Weiwei Gong [a], Pengzhao Gao [a,b,*], Wenxiang Wang [a]

[a] College of Materials Science and Engineering, Hunan University, Changsha 410082, China
[b] Key Laboratory of Low Dimensional Materials & Application Technology of Ministry of Education, Xiangtan University, Xiangtan, Hunan 411105, China

Received 1 July 2010; received in revised form 26 October 2010; accepted 25 January 2011
Available online 9 March 2011

Abstract

A biomorphic porous carbon coated with SiC (SiC/BPC) was prepared by controlled carbonizing native pine under Ar atmosphere and then processed with precursor infiltration-pyrolysis (PIP) of organosilane. Microstructure and component of SiC/BPC were analyzed by FT-IR, XRD, SEM and EDS (attached with line scanning program). The non-isothermal oxidation properties and mechanism of SiC/BPC were studied by TGA. The kinetic parameters were calculated through model-free kinetics methods. Experimental results showed that SiC/BPC had a topologically uniform interconnected porous network microstructure; the obtained gradient SiC coating on BPC surface was amorphous and combined well with the carbon surface, which can improve the oxidation resistance of BPC clearly. The non-isothermal oxidation reaction of SiC/BPC exhibited a partial self-accelerating characteristic. The oxidation process was complicated, firstly it was controlled by gas diffusion in coating, then controlled by chemical reaction, and at last it was controlled by gas diffusion and chemical reaction together, the corresponding effective activation energy was calculated also.

Keywords: Biomorphic porous carbon; SiC gradient coating; Model-free kinetic

1. Introduction

Biomorphic template is a new concept for fabricating ceramic materials with novel hierarchical and complex microstructures using natural biological materials as templates, such as wood [1], rattan [2], rice husk [3] et al. Amongst these, wood has been paid considerable attention with respect to the conversion of its tissue to ceramic materials because it has highly anisotropic cellular structures [4]. Wood has been used to fabricate various novel ceramics with micro-, meso- and macro-structures, classified into the different groups according to the density or porosity of the products [5–7]. Wood-derived cellular ceramics might be of interest for high-temperature-resistant exhaust gas filters, catalyst carriers, advanced micro-reactor systems, immobilization supports for living cells, microbes or enzymes, and waste water treatment, as well as acoustic and heat insulation structures, etc. [8–10]. While, the two factors, the poor oxidation resistance of carbon materials (even at temperatures as low as 700 K), and the weak interface combination of carbon with metal oxide, can effect mechanical properties, function and microstructure of the carbon/oxide ceramics [11]. Ceramic coating, used as a barrier to suppress oxygen diffusion, have been studied [12,13]. A challenge is to find an effective coating to protect carbon materials while being thin enough so as not to crack (due to the thermal mismatch between coating and carbon material). Gradient coating could satisfy above demands [14,15].

However, little work has been done on the oxidation protection of BPC and also the oxidation properties of ceramic coating/BPC has not been studied carefully, which could help to develop more effective oxidation protection for the BPC and also improve the combination of metal oxide and carbon materials. TGA methods (thermogravimetry, differential thermogravimetry) are widely used in the process of studying the oxidation mechanism of carbon materials [15,16]. The results can supply very useful information on the oxidation reaction processes of these kinds of materials and their stability under oxygen atmosphere.

* Corresponding author. Tel.: +86 731 88822269; fax: +86 731 88823554.
E-mail address: gaopengzhao7602@hnu.edu.cn (P. Gao).

0272-8842/$36.00
doi:10.1016/j.ceramint.2011.03.008

In the present work, a biomorphic porous carbon coated with SiC (SiC/BPC) was prepared by controlled carbonizing native pine and then processed with PIP of organosilane. The morphology and composition of SiC/BPC were studied by means of FT-IR, SEM and XRD. The oxidation properties and mechanism of SiC/BPC were studied by non-isothermal TGA.

2. Experimental

2.1. Material preparation

Pine wood was purchased from Changsha Wood Co. (Changsha, China). Wood was shaped, dried at 120 °C for 48 h, and subsequently carbonized under Ar atmosphere with a flow-rate of 50 ml min^{-1} at 1200 °C for 4 h in a graphite heater furnace, resulting in a biomorphic porous carbon template (BPC) [16]. Then, the SiC/BPC was prepared by precursor infiltration-pyrolysis (PIP) of organosilane under a high-purity Ar atmosphere at 1273 K, 30 min at an flow rate of 50 ml/min. The heating rate was 5 °C/min before 400 °C, and 2 °C/min after. By repeating the infiltration-pyrolysis process 1–3 times, three kinds of materials were obtained.

2.2. Characterization and oxidation mechanism experiments

Fourier transform infrared spectroscopy (FTIR) studies were performed with a Fourier transform infrared spectrometer (AVATAR 360 FT-IR, Nicolet) in the wavenumber range of 4000–400 cm^{-1}. The samples' spectra were recorded by transmission in dry air atmosphere through a pastille made of a few milligrams of sample materials mixed with KBr.

The phase component of SiC/BPC was determined by X-ray diffraction (XRD, D5000, Siemens). An X-ray diffractometer using nickel filtered CuK_α radiation produced at 30 kV and 30 mA. Scanning step is 0.01° with 2° min^{-1}.

The micrographs and chemical composition of SiC/BPC (through line scan program) were examined by scanning electron microscopy (SEM, JEOL, JSM-6700F) equipped with an energy dispersive spectrometry (EDS, Oxford).

TGA was performed on thermal analyzer (model Netzsch Thermische Analyzer, STA 409C) with alumina powder as the reference sample. The initial mass of sample was about 7.0 mg.

The oxidation properties and mechanism of BPC and SiC/BPC were measured in air using the same thermal analyzer with a flow-rate of 50 ml min^{-1} and a heating rate of 10, 15 and 25 K min^{-1} from room temperature to 1073 K.

3. Model-free kinetics

Model-free kinetics is based on an iso-conversional computational technique that calculates the effective activation energy (E_a) as a function of the conversion (α) of a chemical reaction, $E = f(\alpha)$. Conversion (α), temperature (T) and time (t) are the three factors influencing the reaction rate of a chemical reaction. The reaction rate represented as function of conversion $f(\alpha)$ is different for each process and must be determined experimentally. The model-free kinetics is a computer program option based on the Vyazovkin and Flynn-Wall-Ozaw theory.

In their approach, no model is applied. The data in this approach is gathered during numerous experiments. The approach follows all points of conversion from multiple experiments instead of a single one [17]. The theory is based on the assumption that

$$\frac{d\alpha}{dt} = k(T)\, f(\alpha) \tag{1}$$

where $f(\alpha)$ represents reaction model and $k(T)$ the Arrhenius rate constant. The activation energy E_a is constant for a certain value of conversion α (this is called iso-conversional method). Taking the reaction rate equation, presented as $f(\alpha)$ and dividing by the heating rate $\beta = dT/dt$, one obtains:

$$\frac{d\alpha}{dt} = k(T)\, f(\alpha) \Rightarrow \frac{d\alpha}{dT} = \frac{k}{\beta} f(\alpha) \tag{2}$$

where $d\alpha/dt$ is the reaction rate (s^{-1}), k the velocity constant (s^{-1}), α the conversion, and β the heating rate (K s^{-1}). Substituting k by the Arrhenius expression $k = k_0\, e^{-E/RT}$ and rearranging gives:

$$\frac{1}{f(\alpha)} d\alpha = \frac{k_0}{\beta} e^{-E/RT}\ dT \tag{3}$$

Integrating up to conversion, α (at the temperature T) gives:

$$\int_0^\alpha \frac{1}{f(\alpha)} d\alpha = g(\alpha) = \frac{k_0}{\beta} \int_{T_0}^{T} e^{-E/RT}\ dT \tag{4}$$

Since $E/2RT \gg 1$, the temperature integral can be approximated by:

$$\int_{T_0}^{T} e^{-E/RT}\ dT \approx -\frac{R}{E} T^2\ \ e^{-E/RT} \tag{5}$$

Substituting the temperature integral, rearranging and logarithmic, one obtains Vyazovkin equation:

$$\ln \frac{\beta}{T_\alpha^2} = \ln\left[\frac{RK_0}{E_a g(\alpha)}\right] - \frac{E_a}{R}\frac{1}{T_\alpha} \tag{6}$$

The Eq. (4) can be rearranged as

$$g(\alpha) = \frac{k_0}{\beta}\int_{T_0}^{T} e^{-E/RT}\ dT = \frac{k_0 E}{\beta R}\int_\infty^u \frac{-e^{-u}}{u^2}\ du = \frac{k_0 E}{\beta R} P(u) \tag{7}$$

where

$$u = \frac{E}{RT} \qquad dT = \frac{E}{Ru^2} du$$

According to Doyle approximation [18], one obtains:

$$\lg\ P(u) = -2.315 - 0.4567 \frac{E_a}{R}\frac{1}{T_a} \tag{8}$$

Combines the Eqs. (7) and (8), one obtains Flynn-Wall-Ozaw equation:

$$\lg\ \beta = \lg\left[\frac{K_0 E_a}{Rg(a)}\right] - 2.315 - 0.4567\frac{E_a}{R}\frac{1}{T_a} \quad (9)$$

The two equations (Eqs. (6) and (9)) are defined as dynamic equation, which are used for the determination of the activation energy for all conversion values (α).

4. Results and discussion

4.1. IR spectrum of SiC/BPC material

Fig. 1 shows the FT-IR spectrum of SiC/BPC. The weak peak at 2966 cm^{-1} belongs to aromatic C–H asymmetrical stretching vibrations (from BPC material) [19], 2894 cm^{-1} is the absorption peak of C–H (belongs to Si–CH_3 or aliphatic) [20]. The peak at 1261 cm^{-1} is attributed to deformed stretching vibration of Si–C, the peak at 1027 cm^{-1} belongs to the stretching vibration of Si–C–Si (belongs to Si–CH_2–Si), and also the peak at 825 cm^{-1} belongs to the stretching vibration of Si–C [20].

The results show that the Si–C bond is obtained and it also exists few of CH_3 or CH_2 groups on the carbon surface for the low pyrolysis temperature.

4.2. Micro-structure of SiC/BPC material

The XRD spectra of BPC and SiC/BPC are shown in Fig. 2. It is obvious that there are two main analogous graphitic peaks corresponding to a broad (0 0 2) peak and a lower intensity (1 0 *l*) peak in the spectrum of BPC. This strongly reveals that BPC is amorphous state and with partly graphitized, and it has a turbostratic microstructure [16]. Three peaks are considered a broad (1 1 1) peak and two lower intensity (2 2 0) and (3 1 1) peaks of β-SiC in the spectrum of SiC/BPC, which exhibits clearly that coating is amorphous state, a not well developed β-SiC [21].

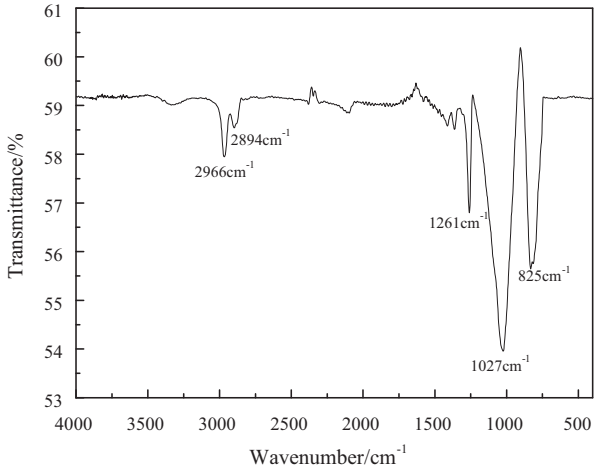

Fig. 1. IR spectrum of SiC/BPC.

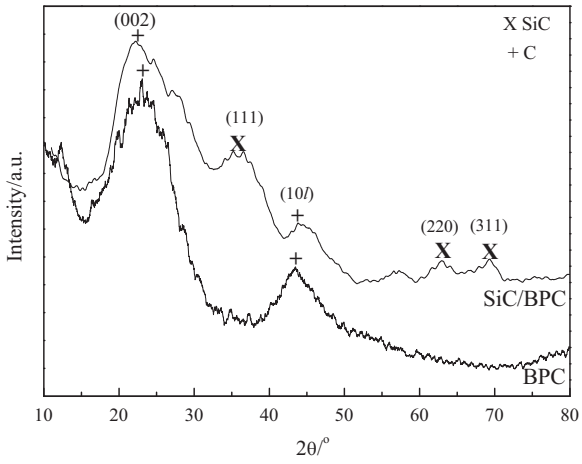

Fig. 2. XRD spectra of BPC and SiC/BPC.

The SEM micrographs of SiC/BPC for different PIP times are shown in Fig. 3. Fig. 3-a exhibits the micrograph of a micro-region of BPC for PIP once and Fig. 3-b exhibits the micrograph of a single wall for the same sample. It can be seen that the microstructure of SiC/BPC shows hollow channels of various diameters that originate from tracheid cells which are parallel to the axis of the tree. Hollow channels of bio-carbon have uniform arrangement, where the black part is lumen and a part is carbon wall. The difference in diameters of hollow channels is attributed to the non-uniform distribution of texture of wood. And also it is easy to see that the uniform coating on carbon surface was obtained and the coating adhered well with surface, there are no cracks.

The line scan spectrum of SiC/BPC (PIP once) is shown in Fig. 3-c (scanning line is shown in Fig. 3-b). In the spectrum, the content of SiC decreases gradually from the edge to the center of carbon wall; contrarily the content of carbon increases gradually. Thus, the gradient SiC coating on carbon wall surface is obtained and the thickness is about 300 nm. According to the results in Fig. 3-b and c, we can draw the conclusion that the uniform gradient coating (SiC) on carbon surface of BPC was prepared and coating adhered well with surface.

Fig. 3-d and e exhibits the micrographs of a single wall for the samples PIP twice and three times. It can be seen clearly that the thickness of coating increases with the increasing PIP times, and some small particles are produced and the size also increases with the PIP times.

4.3. Non-isothermal oxidation properties of SiC/BPC

The TG-DTG curves of BPC and SiC/BPC with different PIP times are shown in Fig. 4. From DTG curves, it is easy to see that the oxidation process of BPC begins from 671 K, but that of SiC/BPC samples are from 797 K, 826 K and 849 K, respectively. From TG curves, it can be seen clearly that BPC burnt out at 862 K, but that of SiC/BPC samples is 938, 997, 1124 K, respectively. These strongly reveal that the oxidation resistance of BPC is improved by SiC coating. And also with

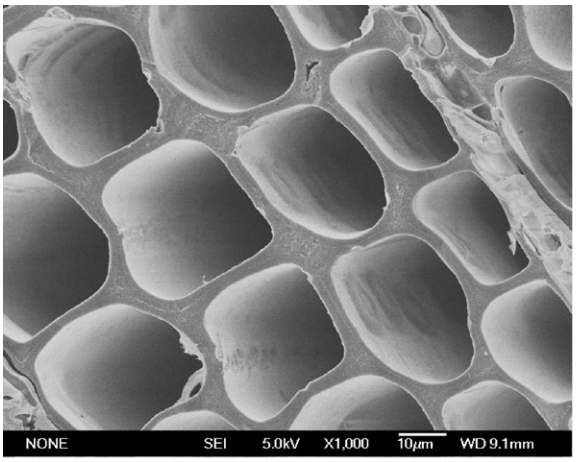

a micro-region of SiC/BPC PIP once

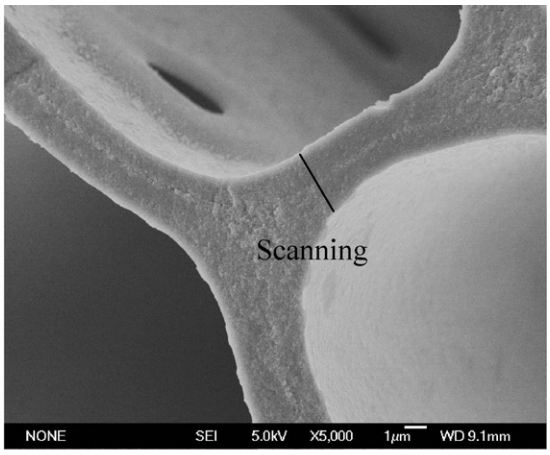

b Single wall of SiC/BPC PIP once

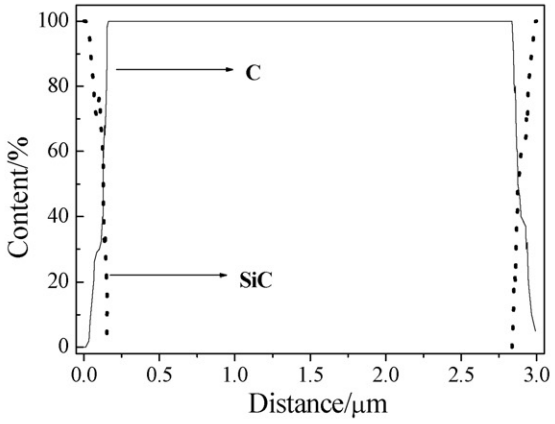

c Line scan spectrum of single wall of SiC/BPC PIP once

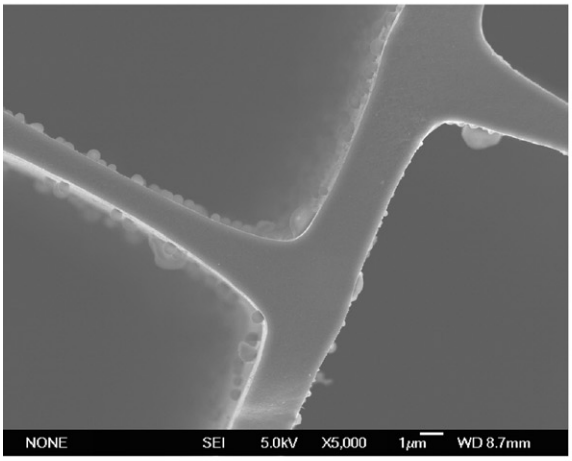

d micro-region of SiC/BPC PIP twice

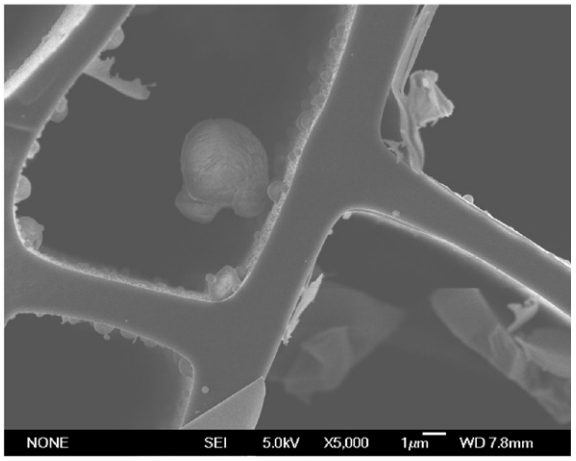

e single wall of SiC/BPC PIP three times

Fig. 3. Micrographs of SiC/BPC with different PIP times.

increasing PIP times, the oxidation resistance properties of BPC increase, resulting from the increase of coating thickness.

From DTG curve, it is easy to see that the oxidation reaction rate ($d\alpha/dT$) is up to the maximum when the SiC/BPC (PIP once) burnt off 32%. Thus, the characteristic of this reaction is a self-accelerating process, according to Ref. [15]. As we know that the microstructure of BPC is turbostratic and has the deformed carbon–carbon multiple circle structure on molecular scale.

Initially, the amount of active carbon atom (ACA, on the edge of carbon–carbon multiple circle, and has unsaturated

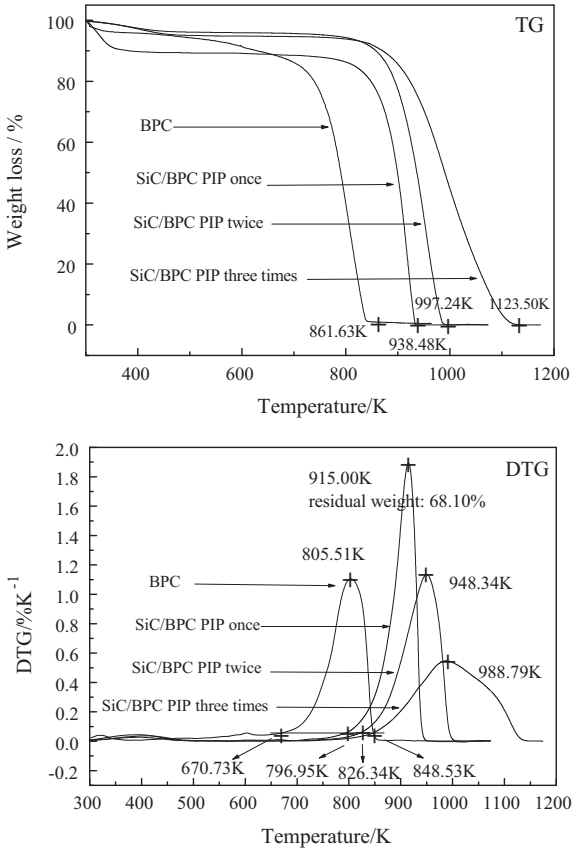

Fig. 4. TG-DTG curves of SiC/BPC with different dipping times (10 K min^{-1}).

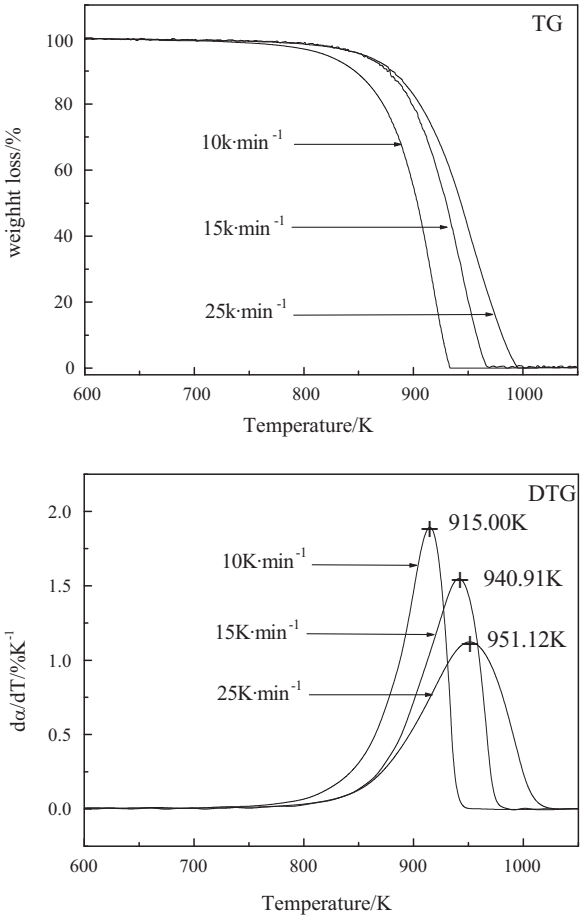

Fig. 5. TG-DTG curves of SiC/BPC (PIP once) with different heating rates.

electronic orbit [16]) on carbon surface is small since the SiC gradient coating exists and also the temperature is low, the SiC/BPC has the lowest oxidation rate. As the oxidation reaction proceeds, the C–C circle of BPC is broken off by the oxidation reaction to produce more ACA when O_2 diffused through the coating and react with carbon, thereby increasing the ACA. Namely, with the increasing of oxidation-weight loss, the amount of ACA increases, the reaction rate increases also. So the self-accelerating characteristic is displayed.

But there is a critical point, when the value of weight loss is bigger than 31.90%, the amount of ACA decreases with the increase of weight loss, the oxidation rate decreases. The characteristic of self-accelerating disappeared. Namely, the non-isothermal oxidation reaction of SiC/BPC exhibits a partial self-accelerating characteristic.

4.4. Non-isothermal oxidation mechanism of SiC/BPC

Model-free kinetics requires at least three dynamic curves with different heating rates. In the present study, three curves of SiC/BPC oxidation reaction with heating rates of 10, 15 and 25 K min^{-1} were determined as shown in Fig. 5. The temperature intervals from 800 to 1000 K are chosen for model-free kinetics calculations.

In accordance with model-free kinetics, for each conversion α, $\ln\ \beta/T_\alpha^2$ was plotted versus $1/T_\alpha$ for Vyazovkin method and $\ln\ \beta$ was plotted versus $1/T_\alpha$ for F-W-O method, giving straight line with the slope $-E_a/R$; therefore the activation energy was obtained as a function of conversion.

By substituting the data obtained from TG-DTG curves in Fig. 5 into Eqs (6) and (9), Fig. 6 presents the E_a of SiC/BPC materials oxidation reaction as a function of conversion percentage α. It can be clearly seen that the E_a value reaches a

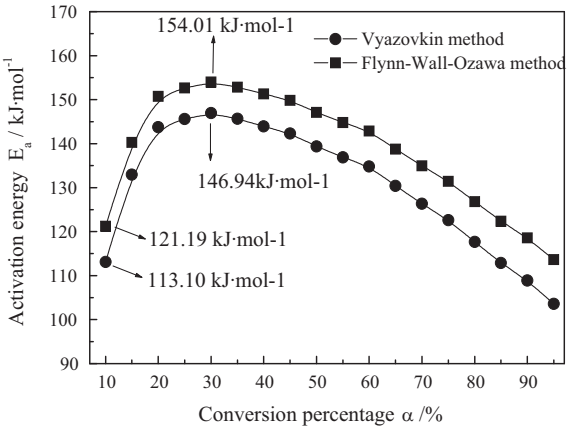

Fig. 6. Change of effective activation energy as a function of conversion percentage for SiC/BPC materials oxidation determined using the model-free methods.

maximum when α equals to 30%. Both curves obtained from Vyazovkin and F-W-O methods have the same tendency.

Vyazovkin has studied the phenomena clearly, the changing E_a value is called "effective E_a". Solid state reactions ordinarily demonstrate a tangled interplay of various chemical and physical processes such as solid-state decomposition, reaction of gaseous products with the solid, sublimation, diffusion, melting, evaporation, etc. Therefore, the effective E_a of a solid state reaction is generally a composite value determined by the E_a of various processes and by their influence on the overall reaction rate, the relative contributions of the elementary steps into the overall reaction rate vary with the extent of conversion ultimately resulting in a dependence of the effective activation energy on the extent of conversion [22–24].

According to Ref. [25] and combined with the above mentioned, it is known that oxidation process of SiC/BPC mainly contains two elementary steps of chemical reaction and gas diffusion, Therefore, the effective E_a of SiC/BPC process is a composite value (Fig. 5) determined by the E_a of the two processes and by their influence on the overall reaction rate, see Eq. (10) [26]:

$$\frac{da}{dT} = f_c(\alpha)k_c(T) + f_d(a)k_d(T) \tag{10}$$

where the subscript c and d stand for chemical reaction and gas diffusion in coating, respectively. Micrographs of SiC/BPC surface with different oxidation weight-losses were shown in Fig. 7.

On the first stage of SiC/BPC oxidation reaction ($\alpha < 25\%$) when α equals to 10%, the temperature is low and only few amount of ACA exists on carbon surface, so the chemical reaction rate is low. But the amount of oxygen diffused through the coating is not enough for the chemical reaction for there is a compact SiC coating existed on carbon surface (see Fig. 7-a). In this condition, gas diffusion shows an important influence on the whole reaction rate ($f_c(\alpha)k_c(T)$) equals near zero, thus the oxidation process of composite is firstly controlled by gas diffusion in coating and the corresponding E_a is about 113–121 kJ mol^{-1}.

As the oxidation reaction proceeds, the α increases. The carbon at the interface of BPC and SiC coating is consumed slowly, which may results that the combination of carbon with coating changes poor. As we know that the coefficient of thermal expanse (CTE) of carbon equals to 7.0×10^{-6} K^{-1} and that value of SiC equals to 4.8×10^{-6} K^{-1}, the uniform coating was broken by the mismatch of thermal expend of carbon and SiC, as can been seen in Fig. 7-b. Namely a few of small crack is produced in coating gradually. So the oxygen diffuses through coating easily than before. At the same time, the temperature increases, more and more ACA is produced on the carbon material surface, which led to the increase of chemical reaction rate. Namely, chemical rate shows an increased influence on the whole reaction rate for the E_a of carbon oxidation reaction equals to 164 kJ mol^{-1} [16], bigger than that of gas diffusion in coating, so the value of E_a increases slowly.

On the second stage ($25 \leq \alpha \leq 35\%$), the temperature increases and the amount of ACA on carbon surface also increases for the self-accelerating characterization of this kinds of materials, the chemical reaction rate also increases. The

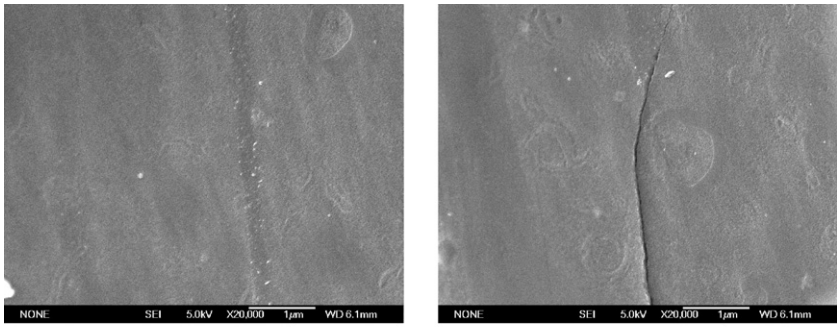

a Oxidation weight-loss 10% b Oxidation weight-loss 30%

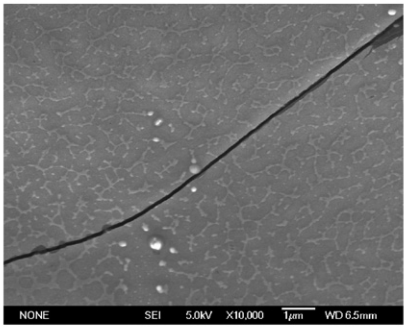

c Oxidation weight-loss 45%

Fig. 7. Micrographs of SiC/BPC surface with different oxidation weight-losses.

oxygen diffused through coating more easily than before for the existed cracks in coating, the content of oxygen diffused through the SiC coating is enough for the chemical reaction. In this condition, the chemical rate shows an important influence on the whole reaction rate ($f_d(\alpha)k_d(T)$ equals to zero approximately), thus the oxidation process of composite is controlled by the chemical reaction and the corresponding E_a is about 154 kJ mol^{-1}, which is similar as the results in Ref. [16].

On the last stage, with the increasing of α, the oxygen diffused through coating easily for more and more cracks are produced in coating (see Fig. 7-c, the same reason see abovementioned). At the same time, although the temperature was high, but the amount of ACA on carbon surface decrease also. In this condition, the oxidation process of SiC/BPC is controlled by chemical reaction and gas diffusion together, and the gas diffusion makes more and more influence on the whole reaction rate (the $f_d(\alpha)k_d(T)$ increases) with the increase of α. For the poor combination of coating, the E_a of gas diffusion in coating decreases, as we know that the E_a of gas diffusion in air is about 15 kJ mol^{-1} [27]. So the effective E_a decreases with the increase of α (Fig. 6) in last stage. At the end, it reaches about 104 kJ mol^{-1}.

5. Conclusions

1. The SiC/BPC has a topologically uniform interconnected porous network microstructure, the obtained gradient SiC coating on BCP surface is amorphous and combined well with the carbon surface, which can improve the oxidation resistance of BPC material clearly. With the increasing of PIP times the oxidation resistance properties of BPC increases resulting from the increase of coating thickness.
2. The non-isothermal oxidation properties of SiC/BPC exhibits a partial self-accelerating characteristic; the reaction rate is up to maximum when the SiC/BPC (PIP once) burnt off 32%.
3. The oxidation process of SiC/BPC shows complicated, first step is controlled by gas diffusion in coating, Second step controlled by chemical reaction, at last it change to control by gas diffusion and chemical reaction together, the corresponding E_a is calculated also.

Acknowledgement

The author thanks for the support of Project (DWKF0805) of Key Laboratory of Low Dimensional Materials & Application Technology of Ministry of Education, Xiangtan University, China.

References

[1] C.R. Rambo, J. Cao, O. Rusina, H. Sieber, Manufacturing of biomorphic (Si, Ti, Zr)-carbide ceramics by sol–gel processing, Carbon 43 (2005) 1174–1183.
[2] A. Zampieri, S. Kullmann, T. Selvam, J. Bauer, W. Schwieger, H. Sieber, T. Fey, P. Greil, Bioinspired rattan-derived SiSiC/zeolite monoliths: preparation and characterisation, Micropor. Mesopor. Mater. 90 (1–3) (2006) 162–174.
[3] V. Martínez, M.F. Valencia, J. Cruz, J.M. Mejía, F. Chejne, Production of β-SiC by pyrolysis of rice husk in gas furnaces, Ceram. Int. 32 (8) (2006) 891–897.
[4] C. Zollfrank, R. Kladny, H. Sieber, Biomorphous SiOC/C ceramic composites from chemically modified wood templates, J. Eur. Ceram. Soc. 24 (2004) 479–487.
[5] A. Hofenauer, O. Treusch, F. Tröger, Dense reaction infiltrated silicon/silicon carbide ceramics derived from wood based composites, Adv. Eng. Mater. 5 (11) (2003) 794–799.
[6] M. Singh, B.M. Yee, Reactive processing of environmentally conscious, biomorphic ceramics from natural wood precursors, J. Eur. Ceram. Soc. 24 (2004) 209–217.
[7] M. Mizutani, H. Takase, N. Adachi, T. Ota, K. Daimon, Y. Hikichi, Porous ceramics prepared by mimicking silicified wood, Sci. Technol. Adv. Mater. 6 (1) (2005) 76–83.
[8] M. Scheffler, P. Colombo (Eds.), Cellular Ceramics: Structure, Manufacturing, Properties and Applications, Willey-VCH Verlag GmbH & Co. KGaA, Weinheim, 2005.
[9] J.P. Borrajo, J. Serra, S. Liste, P. González, S. Chiussi, B. León, M. Pérez-Amor, Pulsed laser deposition of hydroxylapatite thin films on biomorphic silicon carbide ceramics, Appl. Surf. Sci. 248 (1–4) (2005) 355–359.
[10] R.Sh. Vartapetyan, A.M. Voloshchuk, A.K. Buryak, C.D. Artamonova, R.L. Belford, P.J. Ceroke, D.V. Kholine, R.B. Clarkson, B.M. Odintsov, Water vapor adsorption on chars and active carbons–oxygen sensors prepared from a tropical tree wood, Carbon 43 (2005) 2152–2159.
[11] P.Z Gao, H. Wang, Z. Jin, H. Xiao, Influence of coating on the properties of 3-D carbon fiber braid/Al_2O_3 ceramic composite, J. Hunan Univ. (Nat. Sci.) 33 (1) (2006) 86–90.
[12] J.F. Huang, M. Liu, B. Wang, L.Y. Cao, C.K. Xia, J.P. Wang, SiCn/SiC oxidation protective coating for carbon/carbon composites, Carbon 47 (2009) 1189–1206.
[13] X. Zheng, Y. Du, J. Xiao, Y. Lu, C. Liang, Celsian/yttrium silicate protective coating prepared by microwave sintering for C/SiC composites against oxidation, Mater. Sci. Eng. A 505 (2009) 187–190.
[14] J. Li, R.Y. Luo, C. Lin, Y.H. Bi, Q. Xiang, Oxidation resistance of a gradient self-healing coating for carbon/carbon composites, Carbon 45 (2007) 2471–2478.
[15] P.Z. Gao, H.N. Xiao, H.J. Wang, Z.H. Jin, A study on the oxidation kinetics and mechanism of three-dimensional (3D) carbon fiber braid coated by gradient SiC, Mater. Chem. Phys. 93 (2005) 164–169.
[16] P.Z Gao, Y. Bai, S. Lin, W. Guo, H. Xiao, Microstructure properties and non-isothermal oxidation mechanism of biomorphic carbon template, Ceram. Int. 34 (2008) 1975–1981.
[17] I. Majchrzak-Kuceba, W. Nowak, Application of model-free kinetics to the study of dehydration of fly ash-based zeolite, Thermochim. Acta 413 (2004) 23–29.
[18] C.D.J. Doyle, Appl. Polym. Sci. 5 (15) (1961) 285–293.
[19] J.M. Qian, Z.H. Jin, Preparation and characterization of porous, biomorphic SiC ceramic with hybrid pore structure, J. Eur. Ceram. Soc. 26 (2006) 1311–1316.
[20] C.C. Zhou, C.R. Zhang, H.F. Hu, Y.D. Zhang, Z.Y. Wang, Preparation of 3D-C_f/SiC composites at low temperatures, Mater. Sci. Eng. A 488 (2008) 569–572.
[21] K. Jian, Z.H. Chen, Q.S. Ma, H.F. Hu, W.W. Zheng, Effects of pyrolysis temperatures on the microstructure and mechanical properties of 2D-C_f/SiC composites using polycarbosilane, Ceram. Int. 33 (2007) 73–76.
[22] S. Vyazovkin, C.A. Wight, Model-free and model-fitting approaches to kinetic analysis of isothermal and nonisothermal data, Thermochim. Acta 340–341 (1999) 53–68.
[23] S. Vyazovkin, Reply to "What is meant by the term 'variable activation energy' when applied in the kinetics analyses of solid state decompositions (crystolysis reactions)?", Thermochim. Acta 397 (2003) 269–271.

[24] S. Vyazovkin, N. Sbirrazzuoli, Isoconversional analysis of calorimetric data on nonisothermal crystallization of a polymer melt, J. Therm. Anal. Calorim. 72 (2003) 681–686.
[25] R. Luo, Z. Yang, L. Li, Effect of additives on mechanical properties of oxidation-resistant carbon/carbon composite fabricated by rapid CVD method, Carbon 38 (2000) 2109–2115.
[26] J.E.K. Schawe, A description of chemical and diffusion control in isothermal kinetics of cure kinetics, Thermochim. Acta 388 (2002) 299–312.
[27] L.R. Zhao, B.Z. Jang, The oxidation behavior of low-temperature heat-treated carbon fibres, J. Mater. Sci. 32 (1997) 2811–2819.